

The following publication Lv, Q., Lin, Y., Tan, Z., Jiang, B., Xu, L., Ren, H., ... & Chen, S. (2019). Dihydrochalcone-derived polyphenols from tea crab apple (*Malus hupehensis*) and their inhibitory effects on α -glucosidase in vitro. Food & function, 10(5), 2881-2887 is available at <https://doi.org/10.1039/c9fo00229d>.

Dihydrochalcone-derived polyphenols from the crabapple tea (*Malus hupehensis*) and their inhibitory effects on α -glucosidase in vitro

Received 00th January 20xx,
Accepted 00th January 20xx

DOI: 10.1039/x0xx00000x

Qiuyue Lv ^{†a}, Yushan Lin ^{†b}, Zhexu Tan ^a, Baoping Jiang ^a, Lijia Xu ^a, Haiqin Ren ^b, William Chi-shing Tai ^b, Chi-on Chan ^b, Chi-sing Lee ^c, Zhengbing Gu ^d, Daniel K W Mok ^{*b}, Sibao Chen ^{*a,b}

Three dihydrochalcone-derived polyphenols, huperolides A-C (**1-3**), along with thirteen known compounds (**4-16**) were isolated from the leaves of *Malus hupehensis*, the well-known tea crabapple in China. Their chemical structures were elucidated by extensive spectroscopic analysis including NMR (HSQC, HMBC, 1H-1H COSY and ROESY), HRMS and CD spectra. Huperolide A is a polyphenol with a new type of carbon skeleton, while huperolide B, C are a couple of atropisomers, which isolated from natural source for the first time. The antihyperglycemic effects of the isolated compounds were evaluated based on assaying their inhibitory activities against α -glucosidase. As a result, phlorizin (**4**), 3-hydroxyphloridzin (**5**), 3-O-coumaroylquinic acid (**12**) and β -hydroxypropiovanillone (**15**) showed significant concentration-dependent inhibitory effects on α -glucosidase. Therefore, those compounds might be responsible for the antihyperglycemic effect of this herb, and are the most promising compounds to lead discovery of drugs against diabetes.

1. Introduction

Malus hupehensis (Pamp.) Rehd. commonly named as Hupeh crabapple (HPC), Chinese crabapple or tea crabapple, is a Chinese native species of flowering plant in the apple genus *Malus* of the family Rosaceae.¹ Its leaves have been locally used as healthy tea or herbal medicine for the treatment of hyperglycaemia for a long history, especially in Tujia ethnic minority in Hubei Province of China.^{2,3} Owing to its healthy function and safety for human body even after long-time consumption, HPC were lately approved as new food material by National Health Commission of China.⁴ Due to those cause, HPC has been attracting increasing attention by researchers recently. A handful of chemical investigations reported HPC contains flavonoids, phenols and other organic acids.^{2,3,5-8} As in most *Malus* plants, phenols in HPC, such as the dominant compounds phloridzin and 3-hydroxyphloridzin, are chemically derived from dihydrochalcones and responsible for a variety of pharmacological activities.^{9,10} With respect to

biological activity, previous reports revealed that either extractive or pure compounds from HPC exhibited antioxidant,^{3,7} hypolipidemic⁸ and cardioprotective⁵ activities. However, to date, information about the antihyperglycemic chemical components in HPC as well as their biological effects remains limited yet, even though it indeed has been applied to treat type 2 diabetes in folk medicine for a long history. Therefore, it is necessary to explore more active components with unique structure from HPC and evaluate their activities of inhibiting α -glucosidase. In the present study, we conducted comprehensive phytochemical investigation to find more bioactive compounds from HPC. Subsequently, the activities of inhibiting α -glucosidase of isolated compounds were evaluated *in vitro*.

2. Material and methods

2.1 General

Optical rotations were acquired on a Jasco P-2200 digital polarimeter (Jasco Inc., Tokyo, Japan). NMR spectra were measured by Bruker Avance III-400 NMR spectrometer (Bruker Inc., Fällanden, Switzerland). High-resolution ESI-MS (HR-ESI-MS) data were obtained by a Waters Aquity UPLC/Q-TOF mass spectrometer (Milford, MA, USA). Preparative HPLC was applied with a Rainin pump (Rainin Instrument Co. Inc., Woburn, MA, USA), a refractive index detector, and a Cosmosil HPLC column (5C18-MS-II, 10 × 250 mm, Nacalai

^a Institute of Medicinal Plant Development, Peking Union Medical College & Chinese Academy of Medical Sciences, Beijing 100191, People's Republic of China.

^b State Key Laboratory of Chinese Medicine and Molecular Pharmacology (Incubation), The Hong Kong Polytechnic University Shenzhen Research Institute, Shenzhen 518057, People's Republic of China. E-mail addresses: sibao.chen@polyu.edu.hk (S.-B. Chen), Daniel.mok@polyu.edu.hk (Daniel K W Mok).

^c Laboratory of Chemical Genomics, School of Chemical Biology and Biotechnology, Peking University Shenzhen Graduate School, Shenzhen University Town, Xili, Shenzhen 518055, People's Republic of China.

^d Jiangsu Yongjian Medical Technology Ltd., Co. Taizhou 225306, People's Republic of China.

[†] These authors contributed equally to this work.

Tesque, Kyoto, Japan). Silica gel and AB-8 macroporous resin were purchased from Anhui Liangchen Silicon Material Co. Ltd. (Lu'an, Anhui Province, China). Synergy H1 Hybrid Multi-Mode Microplate Reader was from BioTek (VT, USA). α -glucosidase (*Saccharomyces cerevisiae*, G5003, ≥ 10 U/mg), phosphate buffered saline (PBS) (pH 6.8, 0.1 μ M), and acarbose, were purchased from Sigma-Aldrich (St. Louis, MO, USA). *p*-nitrophenyl-D-glucopyranoside (*p*-NPG) was from Tokyo Chemical Industry Co. LTD, (Tokyo, Japan). GraphPad Prism 5.0 was from GraphPad Software, Inc. (La Jolla, CA, USA). Ultra-pure water was prepared with Millipore water purification system (Massachusetts, USA). All other used reagents were analytical grade and purchased from Aladdin (Shanghai, China).

2.2 Plant material

The plant sample was harvested in Yichang city, Hubei Province of China in Sep. 2016, and was authenticated as the leaves of *Malus hupehensis* (Pamp.) Rehd. by Dr. Sibao Chen, one of author of this paper. A voucher specimen (No. HBHT-201609) was deposited in the Institute of Medicinal Plant Development, Peking Union Medical College & Chinese Academy of Medical Sciences.

2.3 Extraction, isolation, and purification procedures

Air-dried leaves of HPC (10 kg) were pulverized to 20 mesh and refluxed with 70% ethanol (2 \times 30 L) for 1.5 h. After filtration and concentrated *in vacuo*, the extracts residual (1.8 kg) was re-dissolved in 2 L water then filtered. The filtrate was subjected to column chromatography (CC) over AB-8 macroporous resin and eluted with 20% and 50% ethanol to get fraction A (401 g) and B (1011 g), respectively. Fraction A (60 g) was subjected to CC over reverse-phase silica gel and eluted with a gradient of ethanol/water (5 to 20%, v/v) to get seven fractions (Fr.1-7). Fr. 1 was subjected to preparative HPLC over RP C-18 (2.0 \times 20 cm, eluted with ACN/0.1% acetic acid (3 : 97, v/v) to obtain compound **2** (100 mg), **3** (50 mg) and **7** (120 mg), respectively. Fr. 4 was subjected to CC over Sephadex LH-20 and eluted with MeOH/H₂O (1 : 9, v/v) to obtain **10** (100 mg) and **16** (100 mg), respectively. Fr. 5 was firstly purified over Sephadex LH-20 column and eluted with MeOH/H₂O (1:9, v/v), further separated by pre-HPLC over RP C-18,

eluted with ACN/0.1% acetic acid (1 : 9, v/v) to gain **6** (1000 mg), **8** (130 mg) and **9** (30 mg), respectively. Fr. 6 was subjected to CC over Sephadex LH-20 and eluted with EtOH/H₂O (12:88, v/v) and then separated by pre-HPLC with eluting solution (10% ACN + 0.1% HAc) to gain **11** (200 mg), **14** (40 mg) and **15** (15 mg), respectively. Fr. 7 was subjected to CC over Sephadex LH-20 and eluted with 3% ethanol and then separated by pre-HPLC with eluting solution (5% ACN + 0.1% HAc) to gain **1** (10 mg), **12** (30 mg) and **13** (80 mg), respectively. Fraction B (60 g) was subjected to CC over Sephadex LH-20 and eluted with gradient of 20% to 50% methanol to get Fr.8-10. Fr. 8 was performed CC by preparative HPLC with elution (30% ACN + 0.1% HAc) to obtain **4** (100 mg) and **5** (100 mg), respectively.

2.4 α -Glucosidase inhibition assay

α -Glucosidase inhibitory activity was determined using a 96-well microtiter plate, with *p*-nitrophenyl-D-glucopyranoside (*p*-NPG) as the substrate, according to a method described previously.¹¹ Briefly, samples were dissolved in phosphate buffered saline (PBS) (pH 6.8, 0.1 μ M) to create a stock test solution (2 mg/mL), respectively, and then diluted with PBS to create series of test solutions with different concentrations for enzyme inhibition test. First, 25 μ L of the test solution was mixed with 5 μ L of the enzyme solution (0.09375 U/mL in PBS pH 7.4). Then, the mixed solution was pre-incubated at 37°C for 5 min. After pre-incubation, 5 μ L of *p*-NPG (3 mM in PBS, pH 7.4) was added and then incubated at 37°C for 30 min. 150 μ L of Na₂CO₃ was added to cease the reaction. The absorbance was measured by a Synergy H1 Hybrid Multi-Mode Microplate Reader at 400 nm for 60 min, recording the absorbance every 5 min. The results were expressed as inhibition percentage by means of the formula described by as follows:¹² Inhibition (%) = $[(A_0 - A_s)/A_0] \times 100$, where A_0 is the absorbance recorded for the enzymatic activity without inhibitor (control), and A_s is the absorbance recorded for the enzymatic activity in presence of the inhibitor (sample). Data were analyzed by using GraphPad Prism 5.0. Acarbose was used as positive control.

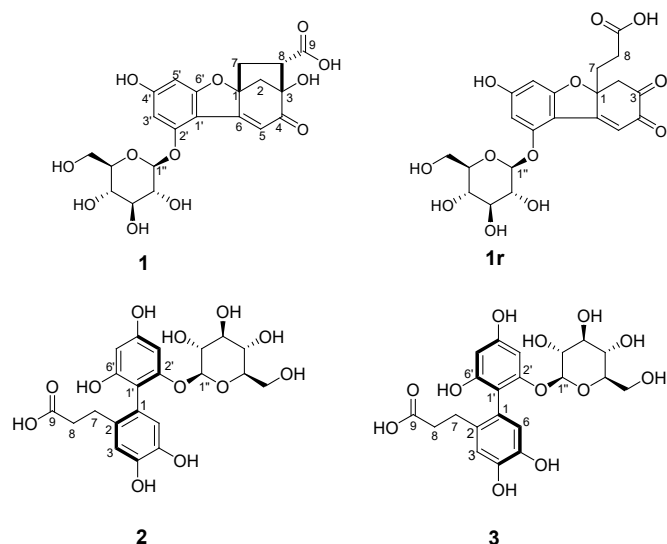


Fig. 1 The chemical structures of compounds **1-3** and **1r**.

3. Results and discussion

3.1 Phytochemical investigation

Compound **1** was obtained as pale-yellowish amorphous powder. The molecular formula was deduced as $C_{21}H_{22}O_{12}$ from HR-ESI-MS (m/z 467.1191 $[M + H]^+$, calcd. 467.1190) analysis and was consistent with 1H and ^{13}C NMR (Table 1) evidence. Signals at δ_H 6.24 (1H, br s, H-3') and 6.13 (1H, br s, H-5') as well as signals at δ_C 96.1 (C-3') and 91.5 (C-5') indicated the presence of a 1,2,3,5-tetrasubstituted aromatic ring. The anomeric signals at δ_H 4.99 (1H, d, $J = 6.5$ Hz, H-1'') and δ_C 99.2 (C-1'') together with the characteristic signals at δ_C 73.1 (C-2''), 76.5 (C-3''), 69.3 (C-4''), 77.1 (C-5'') and 60.4 (C-6'') were attributed to a glucose unit. The remaining 1H and ^{13}C NMR signals of **1** were assigned to a tri-substituted olefin [δ_H 6.22 (1H, s, H-5); δ_C 166.6 (C-6), 107.7 (C-5)] conjugated with a ketone [δ_C 198.2 (C-4)], two fully substituted sp^3 oxygenated carbons [δ_C 91.9 (C-1), 82.0 (C-3)], a methylene group without vicinal protons [δ_H 1.85 (1H, d, $J = 9.6$ Hz, H-2 α), 2.83 (1H, d, $J = 9.6$ Hz, H-2 β); δ_C 46.8 (C-2)], a CH_2CH fragment [δ_H 2.00 (1H, dd, $J = 12.0, 8.2$ Hz, H-7 β) and 2.57 (1H, dd, $J = 12.0, 5.2$ Hz, H-7 α), 2.50 (1H, dd, $J = 8.2, 5.2$ Hz, H-8); δ_C 37.8 (C-7), 45.0 (C-8)], and a carboxyl group (δ_C 173.7). The aforementioned NMR signals indicated that **1** was closely similar with 9-(β -D-glucopyranosyloxy)-2, 3, 4, 4a-tetrahydro-7-hydroxy-2,3-dioxo-4a-dibenzofuranpropanoic acid (**1r**) (Fig. 1), which was reported to have been obtained through

enzymatic oxidation of phloridzin.¹⁰ Compared the NMR data of **1** and **1r** (Fig. 1) reported in literature, the substantial differences between **1** and **1r** are that a ketocarbonyl group and a methylene group in **1r** were replaced by an oxygenated quaternary carbon and a methine in **1**. Considering the biosynthetic pathway of **1**, there should be a carbon-carbon bond between C-3 and C-8. The α -methylene of the carboxyl group attacks the ketone carbonyl in **1r** to form a bridge ring in **1**. In the HMBC spectrum, a long-range correlation (Fig. 2) from δ_H 2.50 (1H, dd, $J = 8.2, 5.2$ Hz, H-8) to δ_C 198.2 (C-4) permitted the speculation. Carefully analysis of the 1D and 2D NMR spectra of **1** revealed that the other parts of the structure were exactly the same as those of **1r**,¹⁰ which were verified by detailed analysis of the HMBC correlations (Fig. 2).

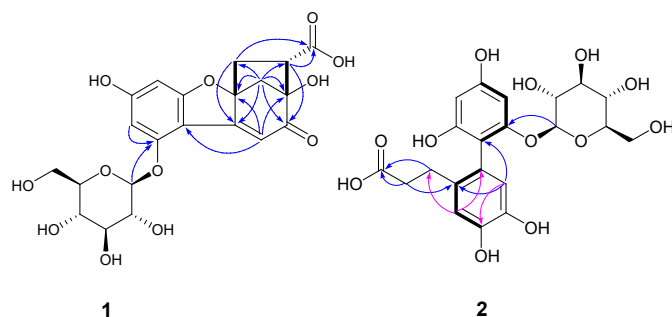


Fig. 2 Significant HMBC correlations of **1** and **2**

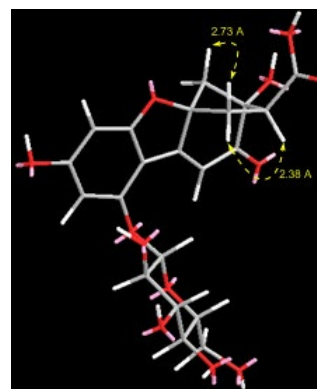


Fig. 3 Significant ROESY correlations of **1**.

Table 1 The NMR data of compounds **1-3** (DMSO-*d*₆, ¹H NMR in 400 Hz & ¹³C in NMR in 100 Hz; δ in ppm, *J* in Hz)

Position	1		1r¹⁰		2		3		2 & 3¹⁰	
	δ ¹ H	δ ¹³ C	δ ¹ H	δ ¹³ C	δ ¹ H	δ ¹³ C	δ ¹ H	δ ¹³ C	δ ¹ H	δ ¹³ C
1	—	91.9	—	89.2	—	124.8	—	124.7	—	124.0
2	1.85 (1H _{α} , d, 9.6) 2.83 (1H _{β} , d, 9.6)	46.8	3.39, 3.32, m	49.9	—	131.3	—	131.3	—	131.4
3	—	82.0	—	192.4	6.55 (1H, s)	115.4	6.57(1H, s)	115.4	6.56, s	115.5
4	—	198.2	—	178.9	—	143.6	—	143.7	—	142.3
5	6.22 (1H, s)	107.7	—	114.7	—	142.3	—	142.4	—	144.0
6	—	166.6	—	165.8	6.35 (1H, s)	119.2	6.39 (1H, s)	118.9	6.36, s	119.3
7	2.00 (1H _{β} , dd, 12.0, 8.2) 2.57 (1H _{α} , dd, 12.0, 5.2)	37.8	2.10, 2.16, m	39.3	2.33-2.47 (2H, m)	27.9	2.34-2.44 (2H, m)	27.8	2.39, 2.46, m	27.9
8	2.50 (1H, dd, 8.2, 5.2)*	45.0	1.84, 2.08, m	28.5	2.22 (2H, t, 8.0)	34.9	2.25 (2H, t, 7.9)	35.0	2.25, m	34.8
9	—	173.7	—	173.4	—	174.7	—	174.7	—	174.7
1'	—	101.8	—	104.1	—	109.1	—	109.2	—	109.2
2'	—	156.9	—	157.7	—	156.4	—	156.5	—	156.5
3'	6.24 (1H, br s)	96.1	6.30, m	97.1	6.06 (1H, d, 2.0)	93.9	6.11(1H, d, 1.9)	94.5	6.05, d, 2.2	96.5
4'	—	166.3	—	167.9	—	157.2	—	157.1	—	157.1
5'	6.13 (1H, br s)	91.5	6.11, m	91.9	6.04 (1H, d, 2.0)	96.4	6.05 (1H, d, 1.9)	94.5	6.07, d, 2.2	94.0
6'	—	166.4	—	167.2	—	155.9	—	156.0	—	155.7
1''	4.99 (1H, d, 6.5)	99.2	4.99, d, 7	100.0	4.68 (1H, d, 7.8)	100.4	4.65 (1H, d, 7.8)	101.0	4.69, d, 7.9	100.4
2''	3.28 (1H, m)**	73.1	3.25, m	69.7	2.91 (1H, dd, 8.9, 7.8)	73.1	2.93 (1H, dd, 8.9, 7.8)	73.4	2.90, m	73.3
3''	3.29 (1H, m)**	76.5	3.34, m	76.9	3.18 (1H, m)	76.8	3.16 (1H, m)	76.6	3.18, m	76.9
4''	3.20 (1H, t-like, 8.8)	69.3	3.35, m	73.4	3.08 (1H, t, 9.2)	69.6	3.08 (1H, t, 9.1)	69.5	3.10, m	69.0
5''	3.34 (1H, br dd, 8.8, 4.4)	77.1	3.38, m	77.4	3.19 (1H, m)	76.9	3.17 (1H, m)	77.0	3.17, m	76.9
6''	3.49 (1H, dd, 11.3, 4.4) 3.67 (1H, br d, 11.3)	60.4	3.52, 3.71, m	60.8	3.47 (1H, dd, 11.8, 5.3) 3.68 (1H, br d, 11.8)	60.7	3.46 (1H, dd, 11.8, 5.2) 3.67 (1H, br d, 11.8)	60.7	3.67, 3.49, m	60.8

*Overlapped signal.

The detectable ROESY correlations (Fig. 3) of H-2 β ↔H-7 α and H-7 β ↔H-8 allowed the assignment of the relative configuration of the bridge ring moiety.

In order to assist the assignment of the absolute configuration of compound **1**, the electronic circular dichroism (ECD) spectrum was recorded. The absolute configuration of **1** was established by the comparison of experimental and calculated ECD spectra of the two isomers **1a** and **1b**. By using the Gaussian 09 software package, the selected conformers were optimized at the B3LYP/6-31G (d, p) level of theory. The theoretical calculations of ECD were performed using time-dependent density functional theory (TD-DFT) at B3LYP/6-31G (d, p) level in MeOH with IEFPCM model. As shown in Fig. 4, the calculated ECD spectra of **1a** matched with the experimental curve. Therefore, the absolute configuration of **1** was determined as 1*R*, 3*R*, 8*S*. Finally, the structure of **1** was established as shown in Fig. 1 and named as huperolide A. Queried by SciFinder, compound **1** represented a new type of carbon skeleton.

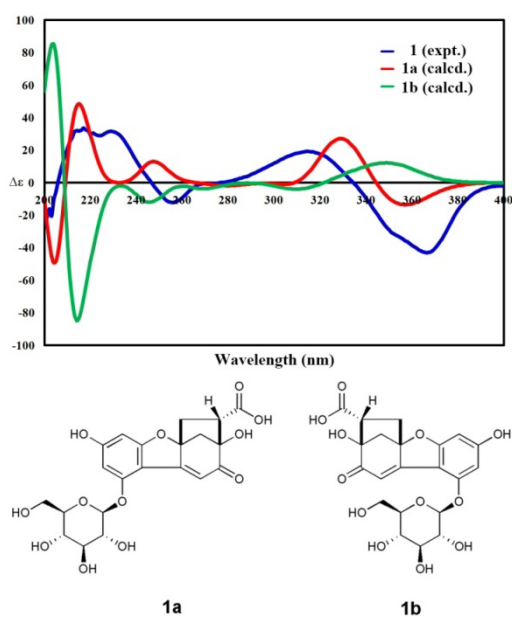


Fig. 4 Structures of **1a** and **1b** and experimentally observed (blue) and theoretically calculated (**1a** red; **1b** green) ECD curves.

Compound **3** was also obtained as a white amorphous powder with rotation $[\alpha]_D^{20}$ –21.2 (c = 0.58, MeOH). Compared with **2**, compound **3** exhibited the same chemical formula and spectral characteristics in terms of MS, 1D and 2D NMR (Table 1), which indicated that **3** possessed the same planar structure with **2**. And the

Compound **2** was obtained as a white amorphous powder with rotation $[\alpha]_D^{20}$ –28.2 (c = 0.89, MeOH). The molecular formula of $C_{21}H_{24}O_{12}$ was determined on the basis of HR-ESI-MS at m/z 491.1162 (calcd. for $C_{21}H_{24}O_{12}Na$, 491.1165) and was consistent with its 1H and ^{13}C NMR data (Table 1), accounting for 10 degrees of hydrogen deficiency. The ion fragment at m/z 307.0829 $[M+H-162]^+$ suggested the presences of a glucose moiety. The 1H NMR spectrum (Table 1) showed the signals for a characteristic anomeric proton signal at δ_H 4.68 (1H, d, J = 7.8 Hz), a 1,2,4,5-tetrasubstituted benzene ring moiety [δ_H 6.55 (1H, s, H-3) and 6.35 (1H, s, H-6)], as well as a 1,2,3,5-tetrasubstituted benzene ring moiety [δ_H 6.06 (1H, d, J = 2.0 Hz, H-3') and 6.04 (1H, d, J = 2.0 Hz, H-5')]. The ^{13}C NMR spectrum (Table 1) showed a total of 21 carbon resonances, comprising one carboxyl carbon (δ_C 174.7), six oxygenated sp^3 carbon signals due to a glucose unit, 12 aromatic carbons from two benzene rings, and two up-field sp^3 methylenes (δ_C 34.9, 27.9) by the DEPT and HSQC analyses. Connectivity of the two tetrasubstituted benzene ring moieties through C-1–C-1' was revealed by the HMBC cross-peaks from δ_H 6.35 (1H, s, H-6) to δ_C 131.3 (C-2), 143.6 (C-4) and 109.1 (C-1'). The presence of a propanoic acid moiety at C-2 was confirmed by the HMBC cross-peaks (Fig. 2) from δ_H 2.33–2.47 (2H, m, H-7) and 2.22 (2H, t, J = 8.0 Hz, H-8) to δ_C 174.7 (C-9), from H-8 to δ_C 131.3 (C-2), and from δ_H 6.55 (1H, s, H-3) to δ_C 124.8 (C-1) and 27.9 (C-7). Furthermore, in the HMBC spectrum, the long-range correlations from δ_H 4.68 (1H, d, J = 7.8 Hz, H-1'') to δ_C (156.4, C-2') allowed us to locate the glucose moiety at C-2'. The glucopyranoside was β -configuration on the ground of a large coupling constant ($^3J_{1'',2''}$ = 7.8 Hz) of the anomeric proton. Therefore, the structure of **2** was established as 3-(4,5,2',4'-tetrahydroxy-6'- β -D-glucopyranosyloxy-[1,1'-biphenyl]-2-yl)propanoic acid, as shown in Fig. 1.

subtle differences between the two compounds were their reverse-phase chromatographic behaviours and chemical shifts in individual places. Further analysis on the structure, the C1–C1' central biaryl axis was found to be restricted due to steric effects of the propionic acid group and glucose moiety. The above information gave us a clear hint that **2** and **3** were a pair of atropo-diastereomers. In order to determine the absolute configuration of the chiral-axis of **2** and **3**, the electronic circular dichroism (ECD) spectra of both isomers were recorded. Absolute configurations of the

two axis isomers were deduced by comparison of their experimental and calculated ECD spectral curves. As shown in Figure 5, compounds **2** and **3** provided nearly mirror-imaged ECD curves. Eventually, the absolute configuration of the chiral-axis of **2** was determined as *P* helicity at C1-C1' axis, while **3** as *M* helicity. Finally, the structures of **2** and **3** were established as shown in Fig. 1 and named as huperolides B and C, respectively. Through literature research, we found that compounds **2** and **3** were previously reported as a mixture derived by enzymatic oxidation of phloridzin with no detailed NMR data¹⁰. Herein, huperolides B and C as monomeric natural products were obtained from nature for the first time, and the absolute configurations of the chiral-

Fig. 5 Experimentally observed (blue) and theoretically calculated (red) ECD curves of **2** and **3**.

axis and complete assignments of the NMR data are also reported for the first time in the current study.

Known compounds were elucidated by comparing their NMR spectroscopic data with those reported in the literature. As a result, **7–11** and **14** were isolated from HPC for the first time.

Phlorizin (**4**),¹⁰ white powder. ¹H-NMR (DMSO, 400

MHz) δ 7.04 (2H, d, *J* = 8.4 Hz), 6.65 (2H, d, *J* = 8.4 Hz), 6.13 (1H, d, *J* = 2 Hz), 5.93 (1H, d, *J* = 2 Hz), 4.95 (1H, m), 3.32 (1H, m), 3.41 (1H, m), 2.75 (2H, t, *J* = 6.4 Hz), 3.31~3.51 (5H, m, H-glu). ¹³C-NMR (DMSO, 100 MHz) δ 205.0, 165.9, 164.9, 161.3, 155.7, 132.0, 129.6 (2C), 115.4 (2C), 105.4, 101.3, 97.4, 94.9, 77.7, 77.2, 73.7, 69.9, 61.0, 45.4, 29.5.

3-hydroxyphloridzin (**5**),¹⁰ white powder. ¹H-NMR (DMSO, 400 MHz) δ 6.75 (1H, d, *J* = 2 Hz), 6.74 (1H, dd, *J* = 8.4, 2 Hz), 6.72 (1H, dd, *J* = 8.4, 2 Hz), 6.70 (1H, d, *J* = 2 Hz), 6.62 (2H, d, *J* = 2 Hz), 3.50 (1H, m), 3.61 (1H, m), 2.85 (2H, t, *J* = 6.4 Hz), 5.01 (1H, m), 3.37~3.52 (6H, m, H-glu). ¹³C-NMR (DMSO, 100 MHz) δ 205.2, 166.1, 164.5, 160.9, 146.3, 144.6, 133.3, 119.3, 117.3, 115.2, 105.5, 100.7, 97.0, 94.1, 77.1, 77.0, 73.3, 69.7, 61.0, 47.7, 29.8.

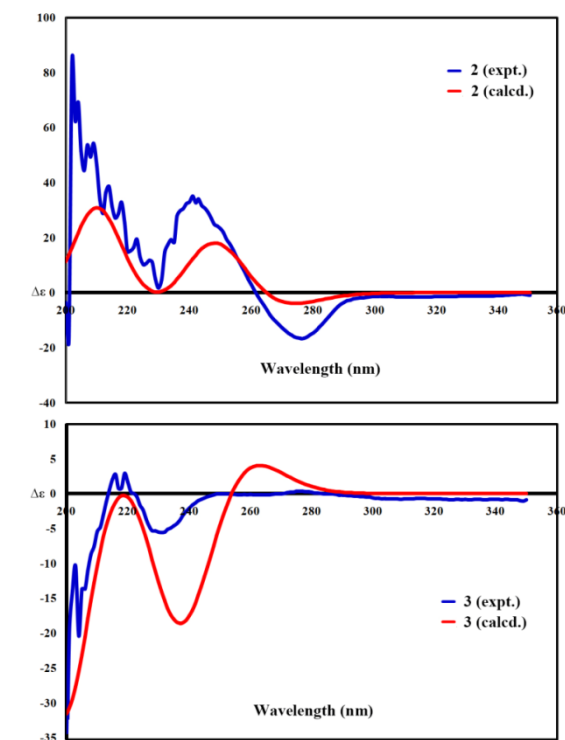
Chlorogenic acid (**6**),^{13, 14} white powder. ¹H-NMR (DMSO, 400 MHz) δ 7.42 (1H, d, *J* = 16 Hz), 6.16 (1H, d, *J* = 16 Hz), 7.04 (1H, d, *J* = 2 Hz), 6.99 (1H, dd, *J* = 8, 2 Hz), 6.77 (1H, d, *J* = 8 Hz), 5.09 (1H, m), 4.89 (1H, m), 3.94 (1H, t, *J* = 3.2 Hz), 1.96~2.05 (4H, m); ¹³C-NMR (DMSO, 100 MHz) δ 175.5, 166.2, 148.8, 146.0, 145.4, 126.1, 121.8, 116.2, 115.2, 114.8, 74.0, 71.4, 71.0, 68.7, 37.7, 36.9.

Protocatechuic acid (**7**),¹⁵ white powder. ¹H-NMR (DMSO, 400 MHz) δ 8.36 (1H, d, *J* = 2 Hz), 8.09 (1H, dd, *J* = 2, 8.4 Hz), 7.33 (1H, d, *J* = 8.4 Hz); ¹³C-NMR (DMSO, 100 MHz) δ 170.2, 152.9, 147.8, 124.8, 124.6, 119.1, 117.0.

Cryptochlorogenic acid (**8**),¹³ white powder. ¹H-NMR (DMSO, 400 MHz) δ 7.51 (1H, d, *J* = 16 Hz), 6.28 (1H, d, *J* = 16 Hz), 7.05 (1H, s), 7.00 (1H, d, *J* = 8.4 Hz), 6.77 (1H, d, *J* = 8.4 Hz), 4.88 (1H, d, *J* = 6.3 Hz), 4.67 (1H, dd, *J* = 3.6, 6.3 Hz), 4.02 (1H, m), 1.91~2.03 (4H, m); ¹³C-NMR (DMSO, 100 MHz) δ 175.7, 166.8, 148.8, 146.1, 145.3, 126.1, 121.7, 116.3, 115.2, 115.1, 77.5, 74.5, 67.0, 64.3, 41.3, 38.1.

6.77 (1H, d, *J* = 8 Hz), 5.20 (1H, m), 4.86 (1H, d, *J* = 4.4 Hz), 3.86 (1H, m), 1.85~2.03 (4H, m). ¹³C-NMR (DMSO, 100 MHz) δ 176.6, 166.5, 148.6, 146.0, 144.9, 126.2, 121.5, 116.3, 115.5, 115.1, 73.4, 71.7, 71.4, 67.8, 38.3, 35.6.

Caffeic acid (**10**),¹³ white powder. ¹H-NMR (DMSO, 400 MHz) δ 7.60 (1H, d, *J* = 16 Hz), 6.32 (1H, d, *J* = 16 Hz), 7.06 (1H, s), 6.96 (1H, d, *J* = 8 Hz), 6.79 (1H, d, *J* = 8 Hz). ¹³C-NMR (DMSO, 100 MHz) δ 167.6, 148.0, 145.4, 145.3, 126.6, 121.5, 115.1, 114.4, 113.7.



Neo-chlorogenic acid (**9**),¹³ white powder. ¹H-NMR (DMSO, 400 MHz) δ 7.46 (1H, d, *J* = 16 Hz), 6.20 (1H, d, *J* = 16 Hz), 7.03 (1H, d, *J* = 2 Hz), 6.97 (1H, dd, *J* = 8, 2 Hz),

p-hydroxy-phenylpropionic acid (**11**),¹⁶ white powder. ¹H-NMR (DMSO, 400 MHz) δ 7.04 (2H, d, J = 8.4 Hz), 6.71 (2H, d, J = 8.4 Hz), 2.82 (2H, t, J = 7.6 Hz), 2.56 (2H, t, J = 7.6 Hz); ¹³C-NMR (DMSO, 100 MHz) δ 175.5, 155.3, 131.5, 128.8 (2C), 114.8 (2C), 35.7, 29.8.

3-*O*-coumaroylquinic acid (**12**),¹⁷ white needle crystal. ¹H-NMR (DMSO, 400 MHz) δ 7.53 (2H, d, J = 8 Hz), 7.50 (1H, d, J = 16 Hz), 6.32 (1H, d, J = 16 Hz), 6.80 (2H, d, J = 8 Hz), 5.11 (1H, m), 4.87 (1H, m), 3.95 (1H, m), 1.78~2.00 (4H, m). ¹³C-NMR (DMSO, 100 MHz) δ 175.7, 166.4, 160.3, 144.9, 130.7 (2C), 125.6, 116.2 (2C), 115.1, 73.8, 71.4, 70.4, 68.4, 37.7, 36.5.

p-coumaric acid (**13**),¹⁸ white powder. ¹H-NMR (DMSO, 400 MHz) δ 7.63 (2H, d, J = 8 Hz), 6.74 (2H, d, J = 8 Hz), 6.67 (1H, d, J = 12.4 Hz), 5.74 (1H, d, J = 12.4 Hz). ¹³C-NMR (DMSO, 100 MHz) δ 168.7, 158.8, 140.4, 132.6 (2C), 126.4, 118.6, 115.3 (2C).

phloroglucinol (**14**),¹⁰ white powder. ¹H-NMR (DMSO, 400 MHz) δ 8.94 (3H, s, OH), 5.66 (3H, s). ¹³C-NMR (DMSO, 100 MHz) δ 159.4 (3C), 94.5 (3C).

β -hydroxypropiovanillone (**15**),¹⁹ white powder. ¹H-NMR (DMSO, 400 MHz) δ 7.51 (1H, d, J = 7.6 Hz), 6.87 (1H, d, J = 7.6 Hz), 7.45 (1H, s), 3.83 (3H, s, OCH₃), 3.76 (2H, t, J = 6 Hz), 3.06 (2H, t, J = 6 Hz). ¹³C-NMR (DMSO, 100 MHz) δ 197.2, 152.1, 148.0, 129.4, 123.5, 115.4, 111.6, 57.7, 56.0, 41.1.

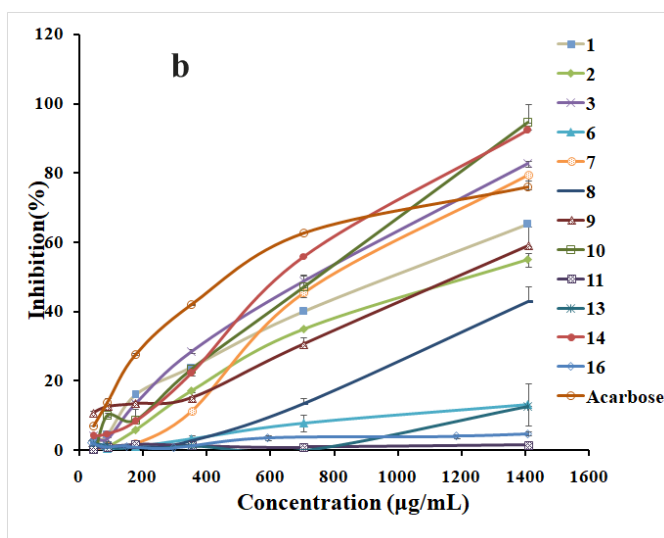
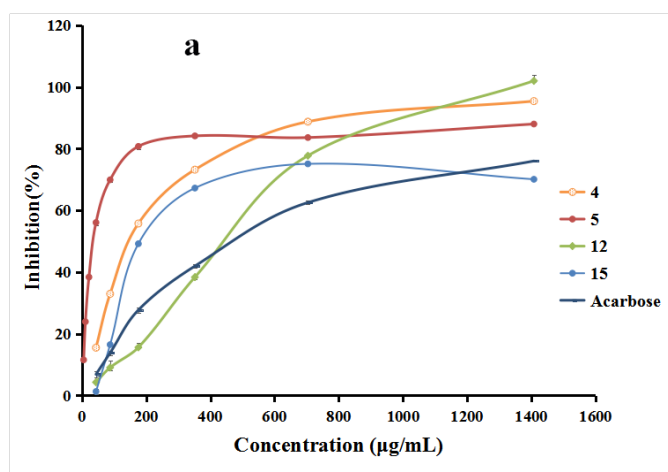
3-hydroxy-1-(4-hydroxy-3,5-dimethoxyphenyl)-1-propanone (**16**),²⁰ white powder. ¹H-NMR (DMSO, 400 MHz) δ 7.25 (2H, s), 3.83 (2H, t), 3.10 (2H, t), 3.78 (6H, s). ¹³C-NMR (DMSO, 100 MHz) δ 197.8, 148.0 (2C), 141.3, 127.9, 106.5 (2C), 57.7, 56.5 (2C), 41.2.

3.2 Inhibitory activity on α -glucosidase

The antihyperglycemic effects of the isolated compounds were evaluated by detecting their inhibition on α -glucosidase with acarbose as positive control. As a result shown in Fig. 6, compared to the positive control, compounds **4**, **5**, **12** and **15** exhibited more significant inhibitory effects in a concentration-dependent manner (Fig. 6a), with the IC₅₀ values of 152.9, 39.03, 406.4 and 257.8 μ g/mL, respectively. Meanwhile, **3**, **7**, **10** and **14** showed similar inhibition of that of acarbose (IC₅₀ = 458.5 μ g/mL) with IC₅₀ values of 641.8, 778.2, 646.0 and 604.6 μ g/mL, respectively, as well as, **1**, **2**, **8** and **9** inhibited α -glucosidase weakly with IC₅₀ values of 897.0, 1175.0, 1598.0 and 1233.0 μ g/mL, respectively (Fig. 6b). However, no inhibition was observed regarding to **6**, **10**, **11** and **13** (Fig. 6b). Therefore, those compounds might be responsible for the hypoglycemic effect of this herb, **4**, **5**, **12** and **15** are the most promising compounds to lead discovery of drugs against diabetes.

4. Conclusions

The present study aimed to discover antihyperglycemic agents from the leaves of *Malus hupehensis* (Pamp.) Rehder (HPC), a well-known healthy tea and folk herb medicine for the treatment of type 2 diabetes in China. As a result, a dihydrochalcone-derived polyphenol with novel carbon skeleton and two naturally occurring atropisomers, together with 13 known compounds were isolated and identified. Meanwhile, the isolated compounds were tested in terms of inhibitory actions against α -glucosidase. As a result, phlorizin (**4**), 3-hydroxyphloridzin (**5**), 3-*O*-coumaroylquinic acid (**12**)



and β -hydroxypropiovanillone (**15**) showed significant concentration-dependent inhibition while compared to the positive control, acarbose. The abovementioned results displayed that like others *Malus* plants, HPC is abundant in polyphenols with chemical diversity. And these polyphenols, particularly phlorizin (**4**), 3-hydroxyphloridzin (**5**) are likely to be effective anti-diabetes components of HPC. Thus, our research revealed HPC is a promising herb for treatment of diabetes, further studies on this herb will probably lead to the discovery of drugs against diabetes.

References

- 1 D. Yv, L. Lu, C. Gu, K. Guan, and W. Jiang, *Flora Republicae Popularis Sinicae*, vol. **36**, Rosaceae (1): *Spiraeoideae-Maloideae*. Beijing: Science Press. 1974.
- 2 Q., Liu, H., Zeng, S., Jiang, L., Zhang, F., Yang, X., Chen, and H. Yang, Separation of polyphenols from leaves of *Malus hupehensis* (Pamp.) Rehder by off-line two-dimensional High Speed Counter-Current Chromatography combined with recycling elution mode, *Food Chem.*, 2015, **186**, 139–45.
- 3 Q. Hu, Y. Chen, Q. Jiao, A. Khan, J. Shan, G. Cao, F. Li, C. Zhang, and H. Lou, Polyphenolic compounds from *Malus hupehensis* and their free radical scavenging effects, *Nat. Prod. Res.*, 2018, **32**, 2152–2158.
- 4 Nation Health Commission of the People's Republic of China. 2014.
- 5 S. Wang, X. Zhu, X. Wang, T. Shen, F. Xiang, and H. Lou, Flavonoids from *Malus hupehensis* and their cardioprotective effects against doxorubicin-induced toxicity in H9c2 cells, *Phytochemistry*, 2013, **87**, 119–125.
- 6 D. Ren, Y. Qin, Y. Yun, H. Lu, X. Chen, and Y. Liang, Using nonrandom two-liquid model for solvent system selection in counter-current chromatography, *J. Chromatogr. A*, 2014, **1355**, 80–85.
- 7 M. Liu, X. Huang, Q. Liu, M. Chen, S. Liao, F. Zhu, S. Shi, H. Yang, and X. Chen, Rapid screening and identification of antioxidants in the leaves of *Malus hupehensis* using off-line two-dimensional HPLC-UV-MS/MS coupled with a 1,1'-diphenyl-2-picrylhydrazyl assay, *J. Sep. Sci.*, 2018, **41**, 2536–2543.
- 8 C. Wen, D. Wang, X. Li, T. Huang, C. Huang, and K. Hu, Targeted isolation and identification of bioactive compounds lowering cholesterol in the crude extracts of crabapples using UPLC-DAD-MS-SPE/NMR based on pharmacology-guided PLS-DA. *J. Pharm. Biomed. Anal.*, 2018, **150**, 144–151.
- 9 P. Sanoner, S. Guyot, N. Marnet, D. Molle, and J. Drilleau, Polyphenol profiles of French cider apple varieties (*Malus domestica* sp.), *J. Agric. Food Chem.*, 1999, **47**, 4847–4853.
- 10 C. L. Guernevé, P. Sanoner, J. F. Drilleau, and S. Guyotb, New compounds obtained by enzymatic oxidation of phloridzin, *Tetrahedron Lett.*, 2004, **45**, 6673–6677.
- 11 Y., Tao, Y., Zhang, Y., Cheng, and Y. Wang, Rapid screening and identification of α -glucosidase inhibitors from mulberry leaves using enzyme-immobilized magnetic beads coupled with HPLC/MS and NMR, *Biomed. Chromatogr.*, 2013, **27**, 148–155.
- 12 C. Choi, S. Lee, and K. Kim, Antioxidant and α -glucosidase inhibitory activities of constituents from *Euonymus alatus* twigs, *Ind. Crop. Prod.*, 2015, **76**, 1055–1060.
- 13 S. Liu, X. Zhou, C. Liang, Q. Zhang, L. Yan, and Z. Wang, Chemical constituents from aqueous extract of *Euodiae Fructus*. *Chin. J. Exp. Trad. Med. Form.*, 2016, **22**, 58–64.
- 14 N. Nakatani, S. Kayano, H. Kikuzaki, K. Sumino, K. Katagiri, and T. Mitani, Identification, quantitative determination, and antioxidative activities of chlorogenic acid isomers in Prune (*Prunus domestica* L.), *J. Agric. Food Chem.*, 2000, **8**, 5512–5516.
- 15 K. N. Scott, Carbon-13 nuclear magnetic resonance of biologically important aromatic acids. I. Chemical shifts of benzoic acid and derivatives, *J. Am. Chem. Soc.*, 1972, **94**, 8564–8568.
- 16 D. Liu, F. Pang, J. Zhang, N. Wang, and X. Yao, Studies on the chemical constituents of *Bulbophyllum odoratissimum* Lindl., *Chin. J. Med. Chem.*, 2005, **15**, 103–107.
- 17 Q. Liang, and L. Ding, Chemical constituents of the hovenia acerba leaves, *Chin. Tradit. Herb. Drug.*, 1997, **28**, 457–459.
- 18 L. Yang, X. Yang, and L. Li, Study on chemical

Fig. 6 *In vitro* α -glucosidase inhibitory effects of isolated compounds from *Malus hupehensis*
*Acarbose was used as positive control.

<http://www.nhfpc.gov.cn/sps/s3585/201409/742b48fc17a847eb90fff31128150269.shtml>.

- constituents of *Lagotis yunnanensis*, *J. Chin. Med. Mat.*, 2005, **28**, 767–768.
- 19 M. Karonen, M. Hämäläinen, R. Nieminen, K. Klika, J. Loponen, V. Ovcharenko, E. Moilanen, and K. Pihlaja, Phenolic extractives from the bark of *Pinus sylvestris* L. and their effects on inflammatory mediators nitric oxide and prostaglandin E2, *J. Agric. Food Chem.*, 2004, **52**, 7532–7540.
- 20 M. Yu, Y. Shao, and Y. Tao, Chemical constituents of Tibetan herbal medicine *Sibiraea laevigata*, *Chin. Tradit. Herb. Drug.*, 2014, **45**, 3528–3531.